L. G. Heller W. H. Chang A. W. Lo

A Model of Charge Transfer in Bucket Brigade and Charge-coupled Devices

Abstract:Investigation of bucket brigade (BB) and charge-coupled devices (CCD) has resulted in the development of a general model for these devices and their various modes of operation. Similarities and differences between BB and CCD are discussed. The nonlinear partial differential equation of charge motion composed of self-induced drift, thermal diffusion, and electrode fringe-field terms is used to study CCD numerically. The factors that affect charge transfer are investigated by varying the stored charge density, the device length, the transfer-gate-to-storage electrode voltage, and the fringe field. The results include several plots of charge transfer vs time.

The FET bucket brigade (BB) and the charge-coupled device (CCD) have been introduced in integrated-circuit form with many possible applications [1-5]. The operation of these surface-charge devices relies on the storage and transfer of mobile charges on a semiconductor surface. Information storage is represented by the presence or absence of a quantity of mobile charges in a metal-oxide-semiconductor capacitor (MOSC) structure or in a metal-oxide-semiconductor junction capacitor (MOSJC) structure for CCD and BB, respectively.

A generalization of CCD operation is depicted in Fig. 1, which shows a cascade of MOSC cells performing as one stage of a shift register. The storage sites are under gates ϕ'_A and ϕ'_B , and the transfer channels are under gates ϕ_A and ϕ_B . During storage, the gate voltages are $\phi_A = \phi_B < \phi'_A = \phi'_B$ and the surface-potential distribution V_b (x) is as shown in Fig. 1(a) when there is no stored charge in the depletion region under the gates. The presence of a quantity of electrons on the semiconductor surface at a storage site (under gate ϕ'_A in the illustration) reduces the surface potential from the reference potential V_R to approximately $V_S = V_R - qn/C$, where $qn = Q_n$ is the magnitude of the stored charge per unit surface area and C is the capacitance of the surface per unit area.

To transfer the stored charges from the storage site under ϕ'_A to the site under ϕ'_B , the gate voltages ϕ_B and

 ϕ_B' are increased. At the start of the transfer, the surface potential distribution is as illustrated in Fig. 1(b). Two distinct modes of operation are possible, depending on the magnitude of the bias potential $V_{\rm ch}$ in the transfer channel. With a channel bias voltage $V_{\rm ch} \ge V_{\rm R}$, all the stored charges at the storage site can be transferred to the next storage site when given sufficient time. At the end of the transfer, all the storage sites under ϕ_A' in the shift register are cleared of stored charges, and thus $V(x) = V_{\rm R}$ under ϕ_A' . This type of operation is the "complete transfer" mode of operation. With a channel bias potential $V_{\rm ch} < V_{\rm R}$, a fixed amount of stored charge $Q_n = C(V_{\rm R} - V_{\rm ch})$ is left behind after the transfer is completed. This is the "residual charge" mode of operation.

The operation of the BB shift register is depicted in Fig. 2, where the storage sites are the n^+ diffused regions at the surface of a p-type substrate. Let us assume that the diffusion "island" under gate ϕ_A is originally chargeneutral, as shown in Fig. 2(a). The application of gate voltage ϕ_B biases the transfer channel (between the two islands) to a potential $V_{\rm ch}$ as indicated in Fig. 2(b). Electrons are transferred from the island under ϕ_A through the transfer channel to the next island, which is biased to a higher potential than $V_{\rm ch}$, until the potential of the island under gate ϕ_A approaches the channel bias potential $V_{\rm ch}$. At the end of the transfer, the surface potential of the receiving site is reduced to $V_S = V_R - qn/C$. Thus

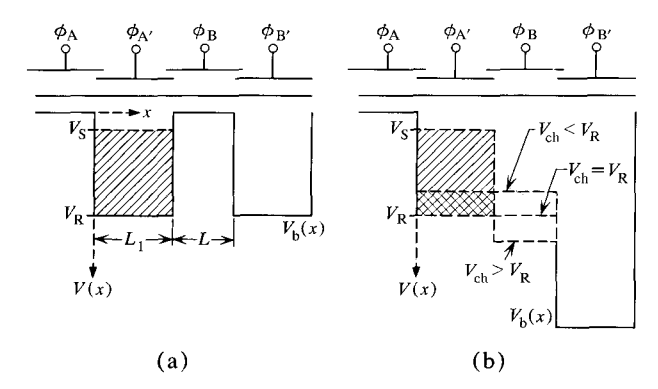


Figure 1 Charge-coupled device (CCD) operation. Surface potential distribution is shown (a) during information storage and (b) at the beginning of charge transfer. The shaded area represents mobile carriers "available" for transfer. Double shading is residual charge for $V_{\rm ch} < V_{\rm R}$.

(a) (b)

Figure 2 Bucket brigade (BB) operation. Surface potential distribution is shown (a) during information storage and (b) at the beginning of charge transfer. Shading has the same meaning as in Fig. 1, except that residual mobile carriers always remain in large quantities because of the nature of the n⁺ storage sites.

the BB shift register operation is essentially identical to the residual charge mode of CCD shift register operation, except for the huge difference in the amount of remaining mobile carriers at the storage site after transfer is completed. Being an n⁺ region with abundant electrons (majority carriers), the storage site of the BB behaves like a conductor, in contrast to the storage site of the CCD which may contain few mobile charges near the end of the transfer.

In both the storage site and the transfer channel of the MOSC or the MOSJC structure, the current per unit length of the surface (perpendicular to the direction of flow) is

$$J_x = q\mu \left(-n\frac{\partial V}{\partial x} + \frac{kT}{q}\frac{\partial n}{\partial x}\right),\tag{1}$$

where μ is the electron mobility and $n=Q_n/q$ is the number of carriers (electrons) per unit area of the surface. By using the approximate relation $V\approx V_{\rm b}-Q_{\rm n}/C$, where C is the surface capacitance per unit area, and neglecting surface state effects, one may express the equation of charge motion as

$$\frac{\partial n}{\partial t} = \mu \left[\frac{q}{C} \frac{\partial}{\partial x} \left(n \frac{\partial n}{\partial x} \right) - \frac{\partial}{\partial x} \left(n \frac{\partial V_b}{\partial x} \right) + \frac{kT}{q} \frac{\partial^2 n}{\partial x^2} \right]. \tag{2}$$

The first term on the right-hand side of this nonlinear partial differential equation represents drift under the influence of the charge-induced field (the concentration gradient of the charged carriers), the second term represents drift under the influence of the electrode fringe field (assumed to be a fixed field for simplicity in computation), and the third term represents thermal diffusion. The implications of assuming a constant fringe field will be dis-

cussed later. Suitable boundary conditions for CCD and BB operation, respectively, are

$$J_x(0,\,t)=0;$$

$$n(L_1+L,\,t)=0$$
 for CCD, and

 $J_x(0,t)=0;$

 $n(L_{2}+L,t)=0;$

$$qL_{2}\frac{dn}{dt}(L_{2},t) = J_{x}(L_{2},t)$$
(4)

for BB. The boundary condition at x=0 implies that no carriers flow backward (to the left), a necessary condition for proper CCD or BB operation. The boundary condition at $x=L_1+L$ or $x=L_2+L$ for CCD or BB, respectively, assumes an infinite limiting velocity. However, this is expected to be a reasonable assumption for the device dimensions used in this study[6].

Numerical solution of the equation of charge motion, with the appropriate boundary and initial conditions, provides a detailed study of charge transfer in these surface charge transfer devices for various modes of operation. Numerical solutions for CCD are illustrated in the following figures. In each figure, the mobile charge distribution n_0 and the bias-potential distribution V_b before the beginning of charge transfer are depicted below the graph. The fraction of the charge remaining at the storage site is plotted vs the transfer time in each graph. Although approximately half the remaining charge in the transfer channel at the end of charge transfer may be transferred back to the storage site when ϕ_B turns off, this effect is not included in the figures. The constants

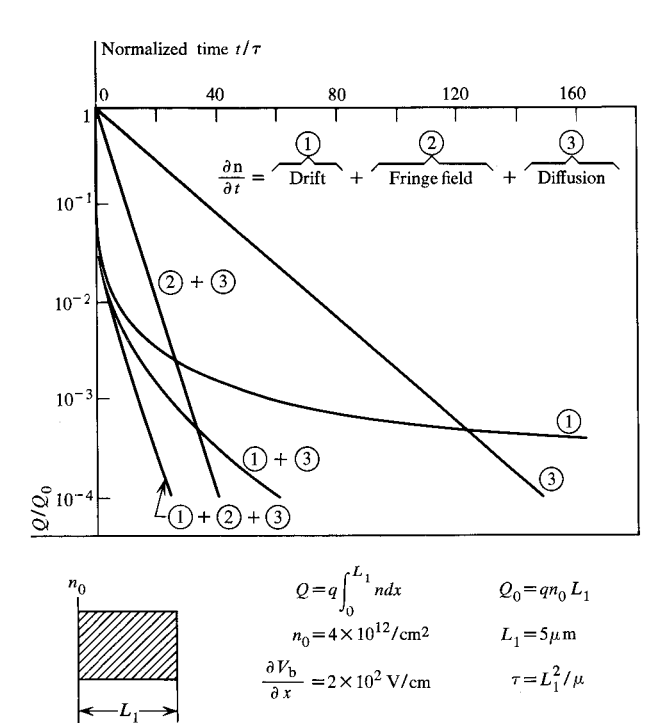


Figure 3 The effect of various components in charge transfer.

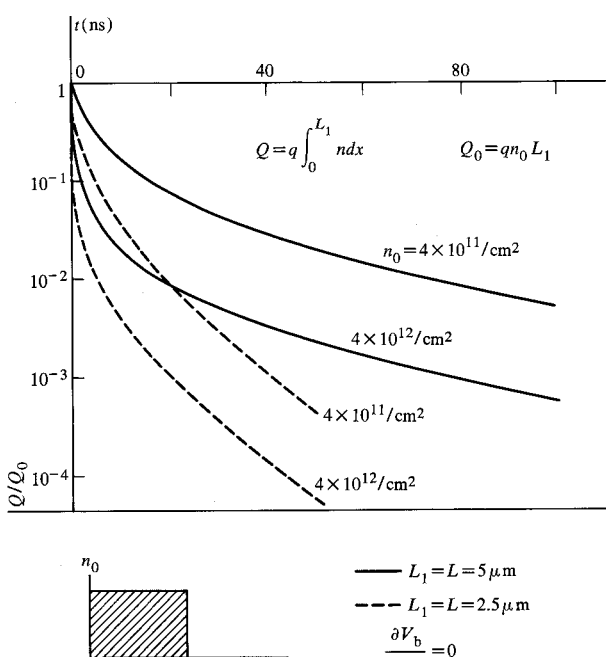
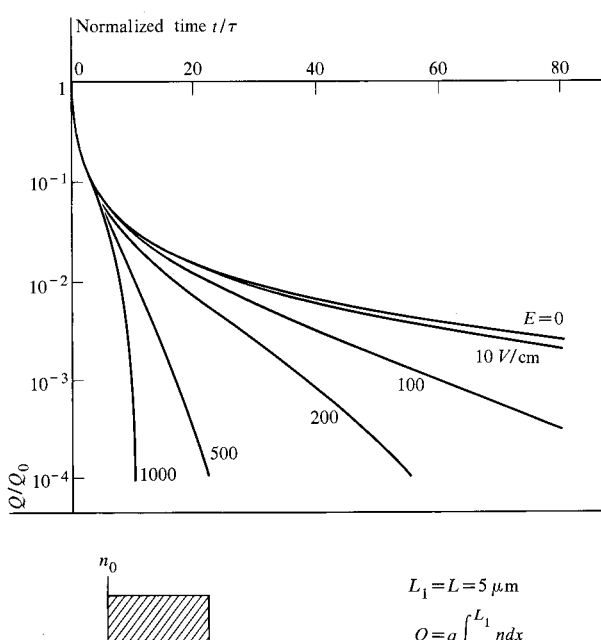


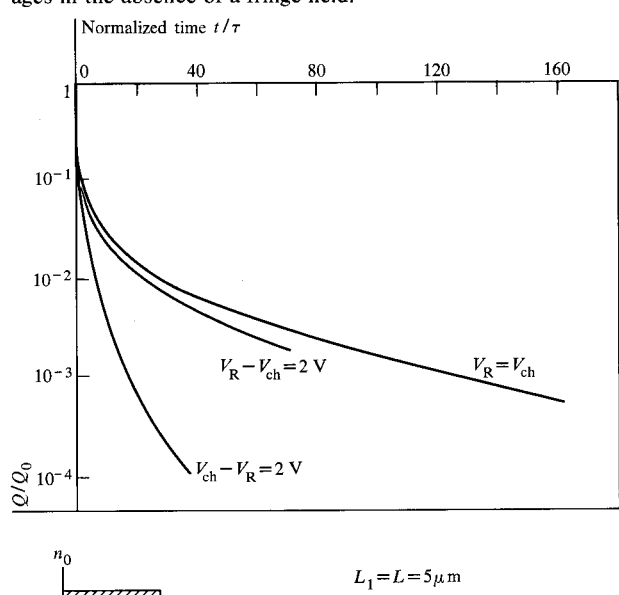
Figure 4 The effect of device length and mobile carrier density in the absence of a fringe field.

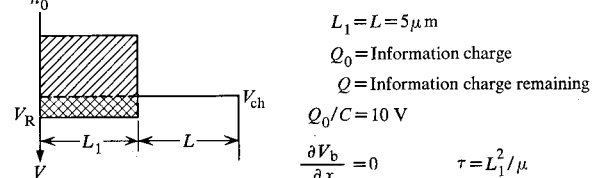
Figure 5 Charge transfer for various fringe field strengths.



 $\tau = L_1^2 / \mu$

Figure 6 Charge transfer for various channel-to-reference voltages in the absence of a fringe field.





used are $\mu = 400 \text{ cm}^2/\text{Vs}$, $q/C = 2.5 \times 10^{-12} \text{ coul-cm}^2/\text{F}$, and kT/q = 0.025 V. The charge transfer is affected by various combinations of the charge-induced drift, fringe field, and thermal diffusion terms as illustrated in Fig. 3. Note that charge-induced drift predominates in the early part of the transfer. The fringe field affects only the "tail" of the transfer where the fields approach a static configuration. Therefore, the original assumption of a constant fringe field throughout transfer is justified. The plot shows that the fringe field and diffusion components yield an exponential time decay in the remaining charge. As shown in Fig. 4, the transfer efficiency improves significantly if the carrier density is increased or if the device length is decreased. The tail of transfer is an exponential of the form $\exp[-Kt/(L_1 + L)^2]$ where K is a constant, as indicated by an earlier report[7]. To achieve a certain Q/Q_0 , the required transfer time as a function of the fringe field strength is as shown in Fig. 5. The charge transfer curves for the cases when $V_{\rm ch} > V_{\rm R}$, $V_{\rm ch} < V_{\rm R}$, and $V_{\rm ch} = V_{\rm R}$ can be observed in Fig. 6. Note that for $V_{\rm ch} - V_{\rm R} = 2$ V the device transfers charge as though the transfer channel were an infinitely deep well.

In conclusion, our numerical results indicate that the transfer efficiency of the CCD improves significantly for higher charge density, shorter device length, higher channel voltage over the reference voltage during charge transfer, and the presence of a fringe field. The residual

charge mode of CCD operation does not substantially improve charge transfer out of the storage site. Although numerical solutions for charge transfer in BB have not been included in this work, CCD and BB have been shown to be conceptually similar.

References

- 1. F. L. J. Sangster, 1970 IEEE International Solid State Circuits Conference Digest, 74 (1970).
- W. S. Boyle and G. E. Smith, Bell System Tech. J. 49, 587 (1970).
- G. F. Amelio, M. F. Tompsett and G. E. Smith, Bell System Tech. J. 49, 593 (1970).
- M. F. Tompsett, G. F. Amelio and G. E. Smith, Appl. Phys. Letters 17, 111 (1970).
- W. E. Engeler, J. J. Tiemann and R. D. Baertsch, Appl. Phys. Letters 17, 469 (1970).
- R. J. Strain and N. L. Schryer, Bell System Tech. J. 50, 1721 (1971).
- 7. C. K. Kim, 1971 IEEE International Solid-State Circuits Conference Digest, 158 (1971).

Received December 1, 1971

L. G. Heller and W. H. Chang are located at the IBM Components Division Laboratory, Burlington (Essex Junction), Vermont 05452. A. W. Lo is currently located at Princeton University, Princeton, New Jersey 08540. His contribution to this paper was done while he was associated with IBM at the Burlington Laboratory.